

Model-Independent Radiative Symmetry Breaking and Gravitational Waves

Alberto Salvio

*Physics Department, University of Rome Tor Vergata,
via della Ricerca Scientifica, I-00133 Rome, Italy*

*I. N. F. N. - Rome Tor Vergata,
via della Ricerca Scientifica, I-00133 Rome, Italy*

Abstract

Models where symmetries are predominantly broken (and masses are then generated) through radiative corrections typically produce strong first-order phase transitions with a period of supercooling, when the temperature dropped by several orders of magnitude. Here it is shown that a model-independent description of these phenomena and the consequent production of potentially observable gravitational waves is possible in terms of few parameters (which are computable once the model is specified) if enough supercooling occurred. It is explicitly found how large the supercooling should be in terms of those parameters, in order for the model-independent description to be valid. It is also explained how to systematically improve the accuracy of such description by computing higher-order corrections in an expansion in powers of a small quantity, which is a function of the above-mentioned parameters. Furthermore, the corresponding gravitational wave spectrum is compared with the existing experimental results from the latest observing run of LIGO and VIRGO and the expected sensitivities of future gravitational wave experiments to find regions of the parameter space that are either ruled out or can lead to a future detection.

Contents

1	Introduction	2
2	General theoretical framework	3
2.1	Radiative symmetry breaking	4
2.2	Thermal effective potential	6
3	Phase transition	8
3.1	An RSB phase transition is always of first order	8
3.2	Supercooling and tunneling	9
4	Gravitational Waves	14
5	Improved approximations	17
6	Summary and conclusions	21

1 Introduction

Current and future gravitational wave (GW) detectors provide us with precious information not only regarding astrophysical systems, such as black holes and other compact objects [1–3], but also in relation to particle physics and the corresponding phenomenology. In particular, they can probe high energies, even higher than those accessible at particle accelerators. A classic example is the fact that strong first-order phase transitions, which are predicted by some Standard Model (SM) high-energy extensions, can generate a background of GWs that may be observable (see Ref. [4] for a textbook introduction). Remarkably, the possible observation of GWs due to a first-order phase transition (PT) would be a clear signal of new physics because the SM does not feature this type of PTs.

The phases that are separated by a PT can have different symmetry properties and some global and/or gauge symmetries can be recovered at high temperatures [5], higher than the critical temperature. In the low-temperature limit these symmetries can be broken by the Higgs mechanism, like in the SM. However, there are other options beyond the SM. One of the most famous alternative is the possibility of breaking some symmetries (and correspondingly generate masses) through radiative (i.e. perturbative loop) corrections. The seminal work on such radiative symmetry breaking (RSB) is Ref. [6] by Coleman and E. Weinberg, which considered a simple toy model (see also Ref. [7] for a recent analysis). The Coleman-Weinberg paper was later extended to a more general field theory by Gildener and S. Weinberg [8]. An important feature of the RSB scenario is approximate scale invariance; radiative corrections generically break this symmetry, but the breaking is small as long as the theory is perturbative.

Many examples of RSB models featuring a strong first-order PT and predicting potentially observable GWs are known. These range from electroweak (EW) symmetry breaking [9–14] to grand unified models [15], passing through, for example, Peccei-Quinn [16] symmetry breaking [17–20] and the seesaw mechanism [21, 22], see Ref. [23] for a review.

The vast number of models where RSB leads to a strong first-order PT and to potentially observable GWs suggests that there may be a model-independent description of these phenomena. Since in works of this type there is typically some degree of supercooling (the temperature drops by several orders of magnitude below the critical temperature before the PT really takes place in the expanding universe), it is natural to conjecture that this phenomenon may play an important and general role. The main objective of this work is to find out if a model-independent proof of the presence of a strong first-order PT exists and, if so, whether there is also a model-independent description of such PT and the consequent GW spectrum. In order to proceed perturbatively, this study also implies an analysis of the validity of the loop and derivative expansions in the general RSB scenario. Another purpose of the present work is to establish whether supercooling is a key and general ingredient for a first-order PT and observable GWs in the RSB scenario.

The consequent theoretical GW spectrum can then be compared, without any need to specify a model, with the constraints and the expected sensitivities of current and future GW experiments. These include ground-based interferometers, such as the advanced Laser Interferometer Gravitational-Wave Observatory (LIGO) [24, 25], Advanced Virgo [26], Cosmic Explorer (CE) [27, 28] and Einstein Telescope (ET) [29–31]) as well as space-based interferometers, like the Big Bang Observer (BBO) [32–34], the Deci-hertz Interferometer Gravitational wave Observatory (DECIGO) [35, 36], the Laser Interferometer Space Antenna (LISA) [37], etc.

An important advantage of the above-mentioned model-independent analysis is of course the fact that one could quickly have information on any given setup once a model is specified, without repeating every time the full analysis of the PT and the GW spectrum.

The paper is structured as follows.

- In Sec. 2 the general theoretical framework of RSB, where the masses are mostly generated radiatively, is analysed. A general number of scalar, fermion and vector fields with arbitrary couplings is considered so that the analysis can be model-independent. In this framework we study the one-loop quantum effective potential and the necessary generation of the EW scale. To reach the main objective of the paper, the corresponding one-loop thermal potential is also studied there.
- In Sec. 3 we study the PT associated with RSB and investigate its nature in full generality. There, the role of supercooling is also considered, again without specifying the model.
- Sec. 4 is then dedicated to the study of the possible GWs produced by the PT in the general RSB scenario and the comparison with the current and future GW detectors.
- To obtain a model-independent description of any phenomenon it is necessary to perform some approximations. The accuracy of these approximations and how to improve them is then discussed in Sec. 5.
- In Sec. 6 a detailed summary of the results of this work as well as the final conclusions are provided.

2 General theoretical framework

Since in the RSB scenario the masses are mostly generated through radiative corrections, we start from the most general no-scale matter Lagrangian describing the interactions between the matter

fields:

$$\mathcal{L}_{\text{matter}}^{\text{ns}} = -\frac{1}{4}F_{\mu\nu}^A F^{A\mu\nu} + \frac{D_\mu\phi_a D^\mu\phi_a}{2} + \bar{\psi}_j i \not{D}\psi_j - \frac{1}{2}(Y_{ij}^a \psi_i \psi_j \phi_a + \text{h.c.}) - V_{\text{ns}}(\phi), \quad (2.1)$$

while gravity is assumed to be described by standard Einstein's theory at the energies that are relevant for this work. Here we consider generic numbers of real scalars ϕ_a , Weyl fermions ψ_j and vectors V_μ^A (with field strength $F_{\mu\nu}^A$), respectively. The V_μ^A are gauge fields and allow us to construct the covariant derivatives

$$D_\mu\phi_a = \partial_\mu\phi_a + i\theta_{ab}^A V_\mu^A \phi_b, \quad D_\mu\psi_j = \partial_\mu\psi_j + it_{jk}^A V_\mu^A \psi_k,$$

where θ^A and t^A are the generators of the (internal) gauge group in the scalar and fermion representations, respectively. Note that, since we are working with real scalars, the Hermitian matrices θ_A are purely imaginary and antisymmetric. The gauge couplings are contained in the θ^A and t^A . Also, the Y_{ij}^a are the Yukawa couplings and $V_{\text{ns}}(\phi)$ is the no-scale potential,

$$V_{\text{ns}}(\phi) = \frac{\lambda_{abcd}}{4!} \phi_a \phi_b \phi_c \phi_d, \quad (2.2)$$

(λ_{abcd} are the quartic couplings). We take λ_{abcd} totally symmetric with respect to the exchange of its indices $abcd$ without loss of generality. In (2.1) all terms are contracted in a gauge-invariant way.

2.1 Radiative symmetry breaking

In the RSB mechanism the mass scales emerge radiatively from loops in a way we discuss now. The basic idea is that, since at quantum level the couplings depend on the RG energy μ , there may be some specific energy at which the potential in Eq. (2.2) develops a flat direction. Such flat direction can be written as $\phi_a = \nu_a \chi$, where ν_a are the components of a unit vector ν , i.e. $\nu_a \nu_a = 1$, and χ is a single scalar field, which parameterizes this direction. Therefore, after renormalization, the RG-improved potential V along the flat direction reads

$$V(\chi) = \frac{\lambda_\chi(\mu)}{4} \chi^4, \quad (2.3)$$

where

$$\lambda_\chi(\mu) \equiv \frac{1}{3!} \lambda_{abcd}(\mu) \nu_a \nu_b \nu_c \nu_d. \quad (2.4)$$

Having a flat direction along ν for μ equal to some specific value $\tilde{\mu}$ means

$$\lambda_\chi(\tilde{\mu}) \equiv \lambda_{abcd}(\tilde{\mu}) \nu_a \nu_b \nu_c \nu_d = 0. \quad (2.5)$$

Besides the potential in (2.3), quantum loop corrections also generate other terms $V_1 + V_2 + \dots$, where V_i represents the i -loop contribution. The explicit expression of V_1 is well known. Here we can recover it, without specifying the details of the underlying theory, by recalling that the effective potential does not depend on μ . Indeed, the renormalization changes the couplings, the

masses and the fields, but leaves the Lagrangian (and in particular the potential) invariant. So we can write

$$\mu \frac{dV_q}{d\mu} = 0, \quad \text{where} \quad V_q \equiv V + V_1 + V_2 + \dots \quad (2.6)$$

Using (2.3), the solution of this equation at the one-loop level is

$$V_q = \frac{\lambda_\chi(\mu)}{4} \chi^4 + \frac{\beta_{\lambda_\chi}}{4} \left(\log \frac{\chi}{\mu} + a_s \right) \chi^4, \quad (2.7)$$

where

$$\beta_{\lambda_\chi} \equiv \mu \frac{d\lambda_\chi}{d\mu} \quad (2.8)$$

is the beta function of λ_χ and a_s is a renormalization-scheme-dependent quantity. Setting now $\mu = \tilde{\mu}$ where $\lambda_\chi = 0$, one obtains

$$V_q(\chi) = \frac{\bar{\beta}}{4} \left(\log \frac{\chi}{\chi_0} - \frac{1}{4} \right) \chi^4, \quad (2.9)$$

where

$$\bar{\beta} \equiv [\beta_{\lambda_\chi}]_{\mu=\tilde{\mu}}, \quad \chi_0 \equiv \frac{\tilde{\mu}}{e^{1/4+a_s}}. \quad (2.10)$$

Note that the renormalization-scheme-dependent a_s has been absorbed in the scale χ_0 . We see that the flat direction acquires some steepness at loop level. The field value χ_0 is a stationary point of V_q . Moreover, χ_0 is a point of minimum when $\bar{\beta} > 0$. Therefore, when the conditions

$$\begin{cases} \lambda_\chi(\tilde{\mu}) = 0 & \text{(flat direction),} \\ \beta_{\lambda_\chi}(\tilde{\mu}) > 0 & \text{(minimum condition),} \end{cases} \quad (2.11)$$

are satisfied quantum corrections generate a minimum of the potential at a non-vanishing value of χ , that is χ_0 . In that case χ_0 is the (radiatively induced) zero-temperature vacuum expectation value of χ and the fluctuations of χ around χ_0 have squared mass $m_\chi^2 = \bar{\beta} \chi_0^2$.

This non-trivial minimum can generically break global and/or local symmetries and thus generate the particle masses, with χ_0 playing the role of the symmetry breaking scale. Consider for example a term in the Lagrangian density \mathcal{L} of the form

$$\mathcal{L}_{\chi h} \equiv \frac{1}{2} \lambda_{ab} \phi_a \phi_b |\mathcal{H}|^2, \quad (2.12)$$

where \mathcal{H} is the Standard Model (SM) Higgs doublet and the λ_{ab} are some of the quartic couplings. RG-improving and setting $\mu = \tilde{\mu}$ and ϕ along the flat direction, ν ,

$$\mathcal{L}_{\chi \mathcal{H}} = \frac{1}{2} \lambda_{\chi h}(\tilde{\mu}) \chi^2 |\mathcal{H}|^2, \quad (2.13)$$

where

$$\lambda_{\chi h}(\mu) \equiv \lambda_{ab}(\mu) \nu_a \nu_b. \quad (2.14)$$

Thus, by evaluating this term at the minimum $\chi = \chi_0$ we obtain the Higgs squared mass parameter

$$\mu_h^2 = \frac{1}{2}\lambda_{\chi h}(\tilde{\mu})\chi_0^2. \quad (2.15)$$

In order to provide a mass to the SM elementary particles, we need $\mu_h^2 > 0$, namely we have the additional condition

$$\lambda_{\chi h}(\tilde{\mu}) > 0 \quad (\text{generation of the EW scale}). \quad (2.16)$$

2.2 Thermal effective potential

In order to write a general formula for the thermal contribution to the effective potential, V_{eff} , we need to write general expressions for the background-dependent masses.

In the scalar sector the elements of the squared-mass matrix are given by the Hessian matrix of the no-scale classical potential in (2.2):

$$M_{S_{ab}}^2 \equiv \frac{\partial^2 V_{\text{ns}}}{\partial \phi_a \partial \phi_b} = \frac{1}{2}\lambda_{abcd}\phi_c\phi_d, \quad (2.17)$$

By evaluating this Hessian matrix at the flat direction $\phi = \nu\chi$ we obtain that the scalar squared-mass matrix M_S^2 is proportional to χ^2 via some quartic couplings, namely

$$M_{S_{ab}}^2(\chi) = \frac{1}{2}\lambda_{abcd}\nu_c\nu_d\chi^2. \quad (2.18)$$

Since M_S^2 is real and symmetric it can be diagonalized with a real orthogonal matrix, to obtain $M_S^2(\chi) \rightarrow \text{diag}(\dots, m_s^2(\chi), \dots)$, where the $m_s(\chi)$ are the background-dependent scalar masses, the eigenvalues of $M_S^2(\chi)$. All the m_s^2 must be non-negative to have a classical potential bounded from below. To prove this first note that the requirement that the classical potential in (2.2) is bounded from below also implies that potential has the absolute minimum at $\phi = 0$ and this minimum vanishes (because no scales are present in (2.2)). Also the classical potential is constantly equal to its value at $\phi = 0$ along the flat direction otherwise that direction would not be flat. So for a classical potential that is bounded from below and has a flat direction $\nu\chi$

$$V_{\text{ns}}(\phi) = V_{\text{ns}}(\nu\chi) + \frac{\partial V_{\text{ns}}}{\partial \phi_a}(\nu\chi)\delta\phi_a + \frac{1}{2}\frac{\partial^2 V_{\text{ns}}}{\partial \phi_a \partial \phi_b}(\nu\chi)\delta\phi_a\delta\phi_b = \frac{1}{2}\frac{\partial^2 V_{\text{ns}}}{\partial \phi_a \partial \phi_b}(\nu\chi)\delta\phi_a\delta\phi_b, \quad (2.19)$$

where $\delta\phi \equiv \phi - \nu\chi$ is taken here infinitesimal. So if there were negative eigenvalues of $M_{S_{ab}}^2(\chi)$ the classical potential would become smaller than its value at the flat direction, but we have seen that this is not possible for a bounded-from-below potential. So all $m_s(\chi)$ must be real and, of course, can be taken non-negative.

This nice property is not shared by theories where symmetry breaking is entirely due to the standard Higgs mechanism, which always requires non-convex regions of the tree-level potential and thus some negative scalar squared masses for some field values.

Let us now turn to the fermion sector. For a given constant field background ϕ , we choose a fermion basis where $\mu_F \equiv Y^a\phi_a$ (as well as μ_F^\dagger) is diagonal, which can be obtained through an $SU(N_F)$ transformation acting on the fermion fields¹. The squared-mass matrix is

$$M_F^2 \equiv \mu_F\mu_F^\dagger. \quad (2.20)$$

¹This is known as the complex Autonne-Takagi factorization, see also Ref. [38].

By evaluating ϕ at the flat direction one obtains $\mu_F(\chi) = Y_\nu \chi$, where $Y_\nu \equiv Y^a \nu_a$, and

$$M_F^2(\chi) = Y_\nu Y_\nu^\dagger \chi^2. \quad (2.21)$$

In our fermion basis $M_F^2(\chi) = \text{diag}(\dots, m_f^2(\chi), \dots)$, where the $m_f(\chi)$ are the background-dependent fermion masses. Given that M_F^2 is the product of μ_F times its Hermitian conjugate all the m_f are real and, of course, can be taken non-negative.

Finally, in the vector sector the elements of the squared-mass matrix M_V^2 are

$$M_{VAB}^2 \equiv \phi^T \theta^A \theta^B \phi, \quad (2.22)$$

and, evaluating at the flat direction, $M_{VAB}^2(\chi) \equiv \nu^T \theta^A \theta^B \nu \chi^2$. Since the θ^A are Hermitian, purely imaginary and antisymmetric, M_V^2 is always real, symmetric and non-negatively defined: one can diagonalize M_V^2 with a real orthogonal matrix, to obtain $M_V^2 \rightarrow \text{diag}(\dots, m_v^2(\chi), \dots)$, where the $m_v(\chi)$ are the background-dependent vector masses, the eigenvalues of $M_V^2(\chi)$, and are, just like the m_s and m_f , all real. Of course, they can also be taken non-negative.

Including the thermal corrections, the general expression of the effective potential V_{eff} is then (in the Landau gauge and at one-loop level)

$$V_{\text{eff}}(\chi, T) = V_q(\chi) + \frac{T^4}{2\pi^2} \left(\sum_b n_b J_B(m_b^2(\chi)/T^2) - 2 \sum_f J_F(m_f^2(\chi)/T^2) \right) + \Lambda_0, \quad (2.23)$$

where $V_q(\chi)$ is given in (2.9), the sum over b runs over all bosonic degrees of freedom and $n_b = 1$ for a scalar degree of freedom (we work with real scalars) and $n_b = 3$ for a vector degree of freedom. In (2.23) the sum over f , which runs over the fermion degrees of freedom, is multiplied by 2 because we work with Weyl spinors. Also, the thermal functions J_B and J_F are defined by

$$J_B(x) \equiv \int_0^\infty dp p^2 \log \left(1 - e^{-\sqrt{p^2+x}} \right) = -\frac{\pi^4}{45} + \frac{\pi^2}{12} x - \frac{\pi}{6} x^{3/2} - \frac{x^2}{32} \ln \left(\frac{x}{a_B} \right) + O(x^3), \quad (2.24)$$

$$J_F(x) \equiv \int_0^\infty dp p^2 \log \left(1 + e^{-\sqrt{p^2+x}} \right) = \frac{7\pi^4}{360} - \frac{\pi^2}{24} x - \frac{x^2}{32} \ln \left(\frac{x}{a_F} \right) + O(x^3). \quad (2.25)$$

In the equations above we also wrote the expansions of $J_B(x)$ and $J_F(x)$ around $x = 0$ modulo terms of order x^3 , where $a_B = 16\pi^2 \exp(3/2 - 2\gamma_E)$, $a_F = \pi^2 \exp(3/2 - 2\gamma_E)$ and γ_E is the Euler-Mascheroni constant (see Ref. [39] for the derivation of those expansions). In Eq. (2.23) we have included a constant term Λ_0 to account for the observed value of the cosmological constant when χ is set to the value corresponding to the minimum of V_{eff} . This addition does not spoil the argument presented above that shows that for a scale-invariant and bounded-from-below potential with a flat direction the eigenvalues of M_S^2 are always non-negative: adding Λ_0 to V_{ns} just produces an additive constant Λ_0 on the right-hand side of Eq. (2.19) and V_{ns} would still be unbounded from below if there were negative eigenvalues of M_S^2 .

Since in the RSB mechanism all m_s^2 , as well as all m_f^2 and m_v^2 , are non-negative the effective potential is real. This is not the case in theories where symmetry breaking occurs through the standard Higgs mechanism: since the tree-level potential is not always convex some of the m_s^2 are necessarily negative and the effective potential acquires an imaginary part. This pathology is a manifestation of the breaking of the (loop) perturbation theory: it occurs because the loop expansion is an expansion around the minima of the scalar action and the regions where the tree-level potential is not convex are too far from those minima. Therefore, the RSB mechanism supports the validity of perturbation theory in the calculation of the effective potential.

3 Phase transition

We are now ready to study the PT associated with a RSB in our general theory (2.1). In field theory the role of the order parameter can be played by the expectation value $\langle\chi\rangle$, which includes quantum as well as thermal averages.

3.1 An RSB phase transition is always of first order

The PT associated with a radiative symmetry breaking is always of first order, namely of the type illustrated in the left plot of Fig. 1, as we now show. First, recall that the definition of RSB implicitly assumes the validity of the perturbative expansion. So in this section we start from this assumption. In Sec. 3.2, however, it will be shown that supercooling (together with, of course, the assumption of small-enough couplings) is sufficient to establish the validity of the one-loop approximation to show that, for the relevant temperatures, there is always a barrier separating the two configurations $\chi = 0$ and $\chi = \chi_0$.

Note that the first three derivatives of the quantum part of the effective potential, $V_q(\chi)$ in (2.9), vanishes at the origin, $\chi = 0$. On the other hand, $J_B(x)$ and $J_F(x)$ feature in their small- x expansion a term linear in x with a coefficient that is positive in J_B and negative in J_F (see Eqs. (2.24) and (2.25)). Since J_B and J_F appear in the effective potential in the way described by Eq. (2.23), this implies that the effective potential has a minimum at the origin, $\chi = 0$, at any non-vanishing temperature. In other words thermal correction renders $\chi = 0$ at least metastable. Going to small enough temperatures the absolute minimum should be approximately the $T = 0$ one given by the potential V_q , but since there is always a positive quadratic term thanks to the finite-temperature contributions the full effective potential always features a barrier between $\chi = 0$ and $\chi = \chi_0$. So the PT is always of first order. Note that this reasoning does not assume the presence of a cubic term, $\sim \chi^3$, in the effective potential, which emerges when bosonic fields are coupled to χ (see Eq. (2.24)), because it also holds when only fermion fields interact with χ .

The absolute minimum of the effective potential is at $\langle\chi\rangle = 0$ for T larger than the critical temperature T_c , while, for $T < T_c$, is at a non-vanishing temperature-dependent value. In the latter case the decay rate per unit of spacetime volume, Γ , of the false vacuum $\langle\chi\rangle = 0$ into the true vacuum $\langle\chi\rangle \neq 0$ occurs via quantum and thermal tunnelling through the barrier and can be computed with the formalism of [40–43]:

$$\Gamma \sim \exp(-S), \quad (3.1)$$

where S is the action

$$S = 4\pi \int_0^{1/T} dt_E \int_0^\infty dr r^2 \left(\frac{1}{2} \dot{\chi}^2 + \frac{1}{2} \chi'^2 + \bar{V}_{\text{eff}}(\chi, T) \right), \quad \bar{V}_{\text{eff}}(\chi, T) \equiv V_{\text{eff}}(\chi, T) - V_{\text{eff}}(0, T) \quad (3.2)$$

evaluated at the bounce, which is the solution of the differential problem [48]

$$\ddot{\chi} + \chi'' + \frac{2}{r} \chi' = \frac{d\bar{V}_{\text{eff}}}{d\chi}, \quad (3.3)$$

$$\dot{\chi}(r, 0) = 0, \quad \dot{\chi}(r, \pm 1/(2T)) = 0, \quad \chi'(0, t_E) = 0, \quad \lim_{r \rightarrow \infty} \chi(r, t_E) = 0. \quad (3.4)$$

Here a dot denotes a derivative with respect to the Euclidean time t_E and a prime denotes a derivative with respect to the spatial radius $r \equiv \sqrt{\vec{x}^2}$. Indeed, the theory at finite T can be formulated as a theory at imaginary time with time period $1/T$ and the boundary conditions in (3.4) impose this periodicity. A particular solution of (3.3)-(3.4) is the time-independent bounce,

$$\chi'' + \frac{2}{r}\chi' = \frac{d\bar{V}_{\text{eff}}}{d\chi}, \quad \chi'(0) = 0, \quad \lim_{r \rightarrow \infty} \chi(r) = 0, \quad (3.5)$$

for which

$$S = \frac{S_3}{T}, \quad S_3 \equiv 4\pi \int_0^\infty dr r^2 \left(\frac{1}{2}\chi'^2 + \bar{V}_{\text{eff}}(\chi, T) \right). \quad (3.6)$$

But generically there could also be time-dependent solutions. When the time-independent bounce dominates the decay rate [42, 43]

$$\Gamma \approx T^4 \left(\frac{S_3}{2\pi T} \right)^{3/2} \exp(-S_3/T). \quad (3.7)$$

Also note that S_3 evaluated at the time-independent bounce can be simplified through the arguments of [44] to obtain

$$S_3 = -8\pi \int_0^\infty dr r^2 \bar{V}_{\text{eff}}(\chi, T). \quad (3.8)$$

Using the expression above instead of the one in (3.6) makes numerical calculations easier because the derivatives of χ do not appear in the action. In general bounce solutions describe the production of bubbles of the true vacuum inside a background of false vacuum.

3.2 Supercooling and tunneling

As long as perturbation theory holds, in a generic theory with RSB, Eq. (2.1), when T goes below T_c the scalar field χ is trapped in the false vacuum $\langle \chi \rangle = 0$ until T is much below T_c , in other words the universe features a phase of supercooling [45]. To understand why this is always the case, note that if the theory is scale invariant Γ must scale as T^4 and, therefore, the smaller T , the smaller Γ . At quantum level, however, scale invariance is broken by perturbative loop corrections, which introduce another dependence of T in the bounce action. This dependence, however, is logarithmic and can become large only when T is very small compared to the other scale of the problem, χ_0 .

We also note that, as a consequence of supercooling, the derivative loop corrections to the effective action can be neglected: at $T = 0$ the quantum effective potential is very shallow because it is only due to perturbatively small loop corrections. So higher-derivative corrections are very small. Also two-derivative and potential loop corrections are suppressed by loop factors. At $T \neq 0$ supercooling implies that for the relevant temperatures the thermal corrections are very small and so V_{eff} is still very shallow and derivative corrections are very small.

Moreover, supercooling tells us that we are far from the high-temperature regime for which the perturbative expansion is known to break down [5, 46, 47], so a one-loop computation should be a good approximation. In particular, it should be noted that the fields that participate in the transition (that directly interact with the flat-direction field χ) receive, thanks to supercooling, a zero-temperature mass that is much larger than the thermal mass and the infrared problem

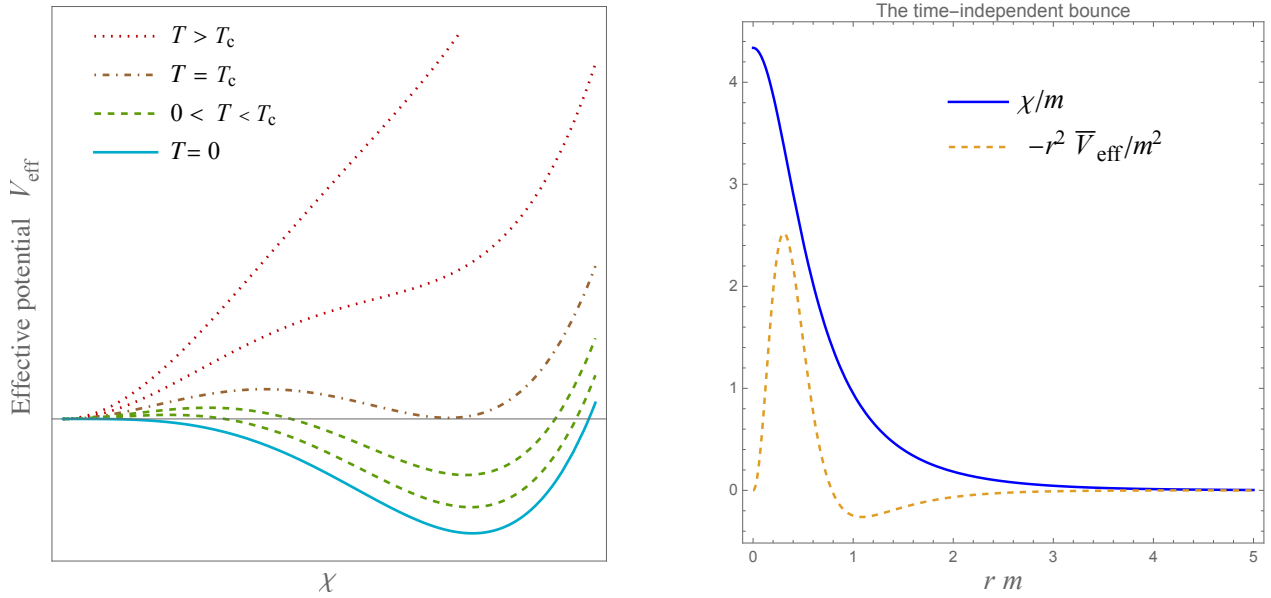


Figure 1: **Left plot:** The temperature-dependent effective potential (including both quantum and thermal contributions) corresponding to a first-order phase transition: the two minima associated with the two phases are separated by a potential barrier; T_c is the critical temperature. **Right plot:** The time-independent bounce and the corresponding integrand function (divided by 8π) appearing in the bounce action, Eq. (3.8), for the effective potential $\bar{V}_{\text{eff}}(\chi) = \frac{m^2}{2}\chi^2 - \frac{\lambda}{4}\chi^4$ and setting $\lambda = 1$.

discussed in [46, 47] is avoided. Therefore, we see that the assumption of supercooling also allows us to be confident about the validity of the one-loop approximation.

Remarkably, if supercooling is strong enough in a generic theory of the form (2.1), to good accuracy², the full effective action for relevant values of χ can be described by three and only three parameters: χ_0 , $\bar{\beta}$ and a real and non-negative quantity g defined as follows:

$$g^2\chi^2 \equiv \sum_b n_b m_b^2(\chi) + \sum_f m_f^2(\chi). \quad (3.9)$$

In other words $g^2\chi^2$ is the sum of all bosonic squared masses plus the sum of all Weyl-spinor squared masses³. All m_b^2 and m_f^2 are real, non-negative and proportional to χ^2 , so g^2 is real, non-negative and independent of χ . Note that g plays the role of a ‘‘collective coupling’’ of χ with all fields of the theory.

We now show the remarkable property mentioned above. First note that the dominant contributions to the bounce action S are those from field values around the barrier. Therefore, we first need to estimate the barrier size, which we can define as the field value χ_b at which V_{eff} equals its value at the false vacuum $\chi = 0$:

$$\bar{V}_{\text{eff}}(\chi_b, T) = 0, \quad (3.10)$$

²The accuracy of the approximation will be analyzed in Sec. 5.

³Note that $g^2\chi^2$ defined in (3.9) does not coincide with the supertrace of the squared-mass matrix because the fermion masses contribute positively in (3.9).

where \bar{V}_{eff} has been defined in Eq. (3.2). Since \bar{V}_{eff} depends on T , the field value χ_b will be a function of T too. Now let us write the logarithmic term in the quantum contribution V_q to V_{eff} , Eqs. (2.9) and (2.23), as follows

$$\log \frac{\chi_b}{\chi_0} - \frac{1}{4} = \log \frac{\chi_b}{T} - \frac{1}{4} + \log \frac{T}{\chi_0}. \quad (3.11)$$

In the presence of supercooling, $T \ll \chi_0$, we expect that neglecting the first two terms in the right-hand-side of Eq. (3.11) is a good approximation because, unlike χ_0 , the field value χ_b clearly becomes small when $T \ll \chi_0$,

$$\log \frac{\chi_b}{\chi_0} - \frac{1}{4} \approx \log \frac{T}{\chi_0}. \quad (3.12)$$

If so, using the expression of the effective potential in (2.9) and (2.23), one finds

$$\frac{\chi_b^4}{T^4} \approx \frac{2}{\pi^2} \frac{J_T(\chi_b^2/T^2) - J_T(0)}{\beta \log \frac{\chi_0}{T}}, \quad (3.13)$$

where

$$J_T(\chi^2/T^2) \equiv \sum_b n_b J_B(m_b^2(\chi)/T^2) - 2 \sum_f J_F(m_f^2(\chi)/T^2). \quad (3.14)$$

The expression in (3.13) tells us that supercooling, $T \ll \chi_0$, suppresses the ratio $\chi_b(T)/T$, but only logarithmically:

$$\frac{\chi_b^4}{T^4} \approx \frac{2}{\pi^2} \frac{J_T(\chi_b^2/T^2) - J_T(0)}{\beta \log \frac{\chi_0}{T}} \approx \frac{2}{\pi^2} \frac{J_T'(0)}{\beta \log \frac{\chi_0}{T}} \frac{\chi_b^2}{T^2} = \frac{g^2}{6\beta \log \frac{\chi_0}{T}} \frac{\chi_b^2}{T^2} \implies \frac{\chi_b^2}{T^2} \approx \frac{g^2}{6\beta \log \frac{\chi_0}{T}}. \quad (3.15)$$

So the approximation in (3.12) is indeed valid. Looking now at the effective potential in (2.23) we see that if the quantity ϵ defined by

$$\epsilon \equiv \frac{g^4}{6\beta \log \frac{\chi_0}{T}} \quad (3.16)$$

is small we can approximate

$$J_B(x) \approx J_B(0) + \frac{\pi^2}{12} x, \quad (3.17)$$

$$J_F(x) \approx J_F(0) - \frac{\pi^2}{24} x, \quad (3.18)$$

where (2.24) and (2.25) have been used. In (3.16) an extra factor g^2 has been inserted compared to (3.15) because χ^2/T^2 appear in the thermal functions multiplied by some coupling constant. Note that the approximations in (3.17) and (3.18) are not valid for all values of χ , including χ_0 , because of supercooling, $T \ll \chi_0$. But, as we have just shown, they are valid for the field values that are important in the bounce action if a large-enough supercooling occurs (ϵ small). This is because in this case $g^2 \chi_b^2/T^2$ is small (see the last equation in (3.15)). Now, using the approximations in (3.12), (3.17) and (3.18), the bounce action can be computed with the effective potential given by

$$\bar{V}_{\text{eff}}(\chi, T) \approx \frac{m^2(T)}{2} \chi^2 - \frac{\lambda(T)}{4} \chi^4 \quad (3.19)$$

where m and λ are real and positive functions of T defined by

$$m^2(T) \equiv \frac{g^2 T^2}{12}, \quad \lambda(T) \equiv \bar{\beta} \log \frac{\chi_0}{T} \quad (3.20)$$

and g^2 is the collective coupling defined in (3.9).

We can now see that the tunneling process is dominated by the time-independent bounce, which satisfies (3.5). The expression of \bar{V}_{eff} in (3.19), together with the form of the bounce problem in (3.3)-(3.4), tells us that the characteristic bounce size R_b is of order $R_b \sim 1/m(T) \gtrsim 1/T$, where in the second estimate we have used the perturbativity condition that g is not too large. This result tells us that the bounce solutions are approximately time-independent (see [42, 43]). Moreover, for a time-dependent bounce the Euclidean action S turns out to be larger than the one of the time-independent bounce for all values of λ and g (at least in the perturbative domain) [48]. This means that the tunneling process is dominated by the time-independent bounce.

At this point we can also note that the gravitational corrections to the false vacuum decay are amply negligible whenever the symmetry breaking scale χ_0 is small compared to the Planck mass M_P , which is, of course, the most interesting case from the phenomenological point of view. This is because, as we have seen, the temperature and the typical scales of the bounce are always much below χ_0 and the gravitational corrections are, therefore, suppressed by factors much smaller than χ_0^2/\bar{M}_P^2 [48], where \bar{M}_P is the reduced Planck mass that is defined in terms of the Planck mass M_P by $\bar{M}_P \equiv M_P/\sqrt{8\pi}$.

Note now that the bounce action S_3 computed with our effective potential in (3.19) is a function of m and λ only, $S_3 = S_3(m, \lambda)$. If we rescale $\chi \rightarrow \chi/\sqrt{\lambda}$ one finds $S_3(m, \lambda) = S_3(m, 1)/\lambda$. Also, using dimensional analysis

$$S_3 = c_3 \frac{m}{\lambda}, \quad (3.21)$$

where c_3 is a dimensionless number: computing explicitly the bounce for $\lambda = 1$ (see the right plot of Fig. 1) and its action through Eq. (3.8) we find

$$c_3 = -\frac{8\pi}{m} \int_0^\infty dr r^2 \left(\frac{m^2}{2} \chi^2 - \frac{1}{4} \chi^4 \right) = 18.8973... \quad (3.22)$$

(see also [49, 50] for previous calculations). This quite large value of c_3 is due to the geometrical factor of 4π overall. The right plot of Fig. 1 shows that for the values of r that give the largest contribution to the bounce action the quartic term is significantly bigger than the quadratic one.

During supercooling the energy density is dominated by the vacuum energy of χ and the universe grows exponentially with Hubble rate $H_I = \sqrt{\bar{\beta}} \chi_0^2 / (4\sqrt{3}\bar{M}_P)$. The bubbles created are diluted by the expansion of the universe and they cannot collide until T reaches the nucleation temperature T_n , which corresponds to $\Gamma/H_I^4 \sim 1$ or, equivalently, using the fact that the decay is dominated by the time-independent bounce,

$$\frac{S_3}{T_n} - \frac{3}{2} \log \left(\frac{S_3/T_n}{2\pi} \right) \approx 4 \log \left(\frac{T_n}{H_I} \right), \quad (3.23)$$

By using the expression of S_3 in (3.21) and the definitions in (3.20) one finds

$$\frac{c_3 g}{\sqrt{12\bar{\beta}} \log \frac{\chi_0}{T_n}} - \frac{3}{2} \log \left(\frac{c_3 g}{2\sqrt{12\pi\bar{\beta}} \log \frac{\chi_0}{T_n}} \right) \approx 4 \log \left(\frac{4\sqrt{3}\bar{M}_P T_n}{\sqrt{\bar{\beta}} \chi_0^2} \right) \quad (3.24)$$

or, equivalently, the approximate equation in X

$$\frac{3}{2}X \log X \approx cX - 4X^2 - a \quad (3.25)$$

having defined

$$X \equiv \log \frac{\chi_0}{T_n} \quad (3.26)$$

and

$$a \equiv \frac{c_3 g}{\sqrt{12\bar{\beta}}}, \quad c \equiv 4 \log \frac{4\sqrt{3}\bar{M}_P}{\sqrt{\bar{\beta}}\chi_0} + \frac{3}{2} \log \frac{a}{2\pi}. \quad (3.27)$$

Recall that g is never negative, the number c_3 has the positive value in (3.22) and $\bar{\beta} > 0$, see (2.11), so a is never negative.

At this point it is important to note that quantities of order $\log X$ has been considered negligible compared to terms of order X in the approximations around Eqs. (3.11)-(3.15). To be consistent with these approximations we drop the term $\frac{3}{2}X \log X$ in (3.25):

$$cX - 4X^2 - a \approx 0. \quad (3.28)$$

Here we are interested in the solution of Eq. (3.28) with the smaller X , which corresponds to Γ reaching H_I^4 from below. This solution gives

$$T_n \approx \chi_0 \exp\left(\frac{\sqrt{c^2 - 16a - c}}{8}\right). \quad (3.29)$$

Note that in the decoupling limit ($g \rightarrow 0$, $\bar{\beta}/g \rightarrow 0$ and χ_0 fixed) $\sqrt{a} \rightarrow \infty$ faster than $c \sim \log a$ and there is no solution for T_n . This occurs because in this limit $\Gamma \rightarrow 0$ and so can never be of order H_I^4 . As a result, the existence of a solution of Eq. (3.28), which determines T_n , requires a minimum value of the collective coupling g , such that $c^2 \geq 16a$; however, the smaller g (at $\bar{\beta}/g^4$ fixed) the larger $\log(\chi_0/T_n)$ and the universe supercools more, at least for realistic and perturbative values of the parameters. Moreover, in general supercooling is also enhanced by increasing χ_0 at g and $\bar{\beta}$ fixed, although this effect is very mild as c depends on χ_0 only logarithmically. In Sec. 5 we will discuss the accuracy of the approximations performed in this section and explain how to improve them.

One might wonder whether the effect of the spacetime curvature due to $H_I \neq 0$ can alter the decay rate. In standard Einstein gravity, this may happen if T_n is so small to be comparable with H_I . We checked that, whenever a solution for T_n exists, this never happens, at least for realistic and perturbative values of the parameters. On the other hand, if a solution for T_n does not exist the effect of the spacetime curvature, as well as quantum fluctuations, can eventually become important in the decay rate [17, 51–53].

In general, the strength of the PT is measured by the parameter α defined as the ratio between

$$\rho(T_n) \equiv \left[\frac{T}{4} \frac{d}{dT} \bar{V}_{\text{eff}}(\langle \chi \rangle, T) - \bar{V}_{\text{eff}}(\langle \chi \rangle, T) \right]_{T=T_n} \quad (3.30)$$

and the energy density of the thermal plasma (see [54, 55] for more details). In (3.30) $\langle \chi \rangle$ is the point of absolute minimum of the effective potential, which at $T = T_n$ is not zero. By definition α is

$$\alpha \equiv \frac{30\rho(T_n)}{\pi^2 g_*(T_n) T_n^4}, \quad (3.31)$$

where $g_*(T)$ is the effective number of relativistic species at temperature T . In the presence of supercooling we then typically have

$$\rho(T_n) \approx [-\bar{V}_{\text{eff}}(\langle\chi\rangle, T)]_{T=T_n}. \quad (3.32)$$

Moreover,

$$\alpha \gg 1, \quad (3.33)$$

because the energy density is dominated by the vacuum energy of χ , as we have seen. So in the RSB scenario one has a very strong PT.

4 Gravitational Waves

In the RSB scenario the dominant source of GWs are bubble collisions that take place in the vacuum. This is because the energy density of the space where the bubbles move are dominated by the vacuum energy density associated with χ , which leads to an exponential growth of the corresponding cosmological scale factor as we have seen. This inflationary behavior as usual dilutes preexisting matter and radiation and, therefore, we neglect the GW production due to turbulence and sound waves in the cosmic fluid [4, 56, 57].

An important parameter to analyse the spectrum of the GWs is the inverse duration β of the PT that, in models with supercooling, is given by [56, 58, 59]

$$\beta = \left[\frac{1}{\Gamma} \frac{d\Gamma}{dt} \right]_{t_n}, \quad (4.1)$$

where t_n is the value of the time t when $T = T_n$. Using then $dt = -dT/(TH(T))$, where $H(T)$ is the Hubble rate corresponding to the temperature T , and the fact that the tunneling process is dominated by the time-independent bounce,

$$\beta \approx H_n \left[T \frac{d}{dT} (S_3/T) - 4 - \frac{3}{2} T \frac{d}{dT} \log(S_3/T) \right]_{T=T_n}, \quad (4.2)$$

where $H_n \approx H_I$ is the Hubble rate when $T = T_n$.

Now, if supercooling is large enough that one can use the expression of S_3 in (3.21), one obtains

$$\frac{\beta}{H_n} \approx \frac{a}{\log^2(\chi_0/T_n)} - 4 - \frac{3}{2} \frac{1}{\log(\chi_0/T_n)}, \quad (4.3)$$

where a is defined in terms of $\bar{\beta}$ and g in (3.27). The last term in the expression above, which corresponds to the last term in (4.2), can be neglected as χ_0/T_n is very large. However, the first term $a/\log^2(\chi_0/T_n)$ generically cannot be neglected because the coefficient a is typically very large as $\bar{\beta}$ is loop suppressed and c_3 is larger than 10, see (3.22). So

$$\frac{\beta}{H_n} \approx \frac{a}{\log^2(\chi_0/T_n)} - 4. \quad (4.4)$$

Eq. (4.4) then explicitly indicates that the PT lasts more when T_n/χ_0 is smaller. Inserting the expression of T_n given in (3.29) into (4.4), one obtains β/H_n in terms of χ_0 , $\bar{\beta}$ and g .

From [56] we find the following GW spectrum due to vacuum bubble collisions⁴ (valid in the presence of supercooling and $\alpha \gg 1$)

$$h^2\Omega_{\text{GW}}(f) \approx 1.29 \times 10^{-6} \left(\frac{H_r}{\beta}\right)^2 \left(\frac{100}{g_*(T_r)}\right)^{1/3} \frac{3.8(f/f_{\text{peak}})^{2.8}}{1 + 2.8(f/f_{\text{peak}})^{3.8}}, \quad (4.6)$$

where T_r is the reheating temperature after supercooling, H_r is the corresponding Hubble rate and f_{peak} is the red-shifted frequency peak today, which is given by [56]

$$f_{\text{peak}} \approx 3.79 \frac{\beta}{H_r} \left(\frac{g_*(T_r)}{100}\right)^{1/6} \frac{T_r}{10^8 \text{GeV}} \text{ Hz}. \quad (4.7)$$

Ref. [56] used, among other things, the results of [60] based on the envelope approximation. This is an approximation where all the energy is assumed to be stored in the bubble walls, which are taken to be thin, and, as the bubbles collide, one uses as a source for GW production the energy-momentum tensor of the uncollided part of the bubble walls. In our situation this is expected to capture the dominant source of GWs [61] because, during the exponential growth of the universe, the bubbles expand considerably and in this process the energy gained in the transition from the false to the true vacuum is transferred to the bubble walls, which, at the same time, become thinner⁵.

Eq. (4.6) shows that the GW spectrum is larger for smaller values of β . So an approximate scale invariance, which, as we have seen, can suppress β , can also lead to strong GW signals; the larger the supercooling is the stronger the GW signals are. For sufficiently fast reheating, which might occur e.g. thanks to the Higgs portal coupling in (2.13),

$$H_r \approx H_n \approx H_I, \quad \text{and} \quad T_r^4 \approx \frac{15\bar{\beta}\chi_0^4}{8\pi^2 g_*(T_r)}. \quad (4.8)$$

But otherwise H_r and T_r can depend on the details of the specific model.

Note that any cosmic source of GW background acts as an extra radiation component and is highly constrained by big-bang nucleosynthesis (BBN) measurements of primordial elements [67–69]. The measurement of the effective number of neutrino species N_{eff} and the observational abundance of deuterium and helium, leads to the following bound [4]:

$$\int_{f_{\text{BBN}}}^{f_{\text{UV}}} \frac{df}{f} h^2\Omega_{\text{GW}}(f) < 1.3 \times 10^{-6} \frac{N_{\text{eff}} - 3.046}{0.234}, \quad (4.9)$$

where $f_{\text{BBN}} \sim 10^{-11} \text{Hz}$ (see e.g. [4, 67]) and f_{UV} is some UV cutoff, which can be conservatively taken to be around \bar{M}_P . In the right-hand-side of (4.9) we can use the reference value $N_{\text{eff}} = 2.99 + 0.17 = 3.16$, which corresponds to the most precise experimental upper bound on N_{eff} published by the Planck collaboration in 2018 [70].

⁴The spectral density Ω_{GW} is defined as usual by

$$\Omega_{\text{GW}}(f) \equiv \frac{f}{\rho_{\text{cr}}} \frac{d\rho_{\text{GW}}}{df}, \quad (4.5)$$

where $\rho_{\text{cr}} \equiv 3H_0^2 \bar{M}_P^2$ is the critical energy density, H_0 is the present value of the Hubble rate and ρ_{GW} is the energy density carried by the stochastic background.

⁵See, however, the recent works [62–66] that improved the calculation of Ω_{GW} and can be relevant in the general case.

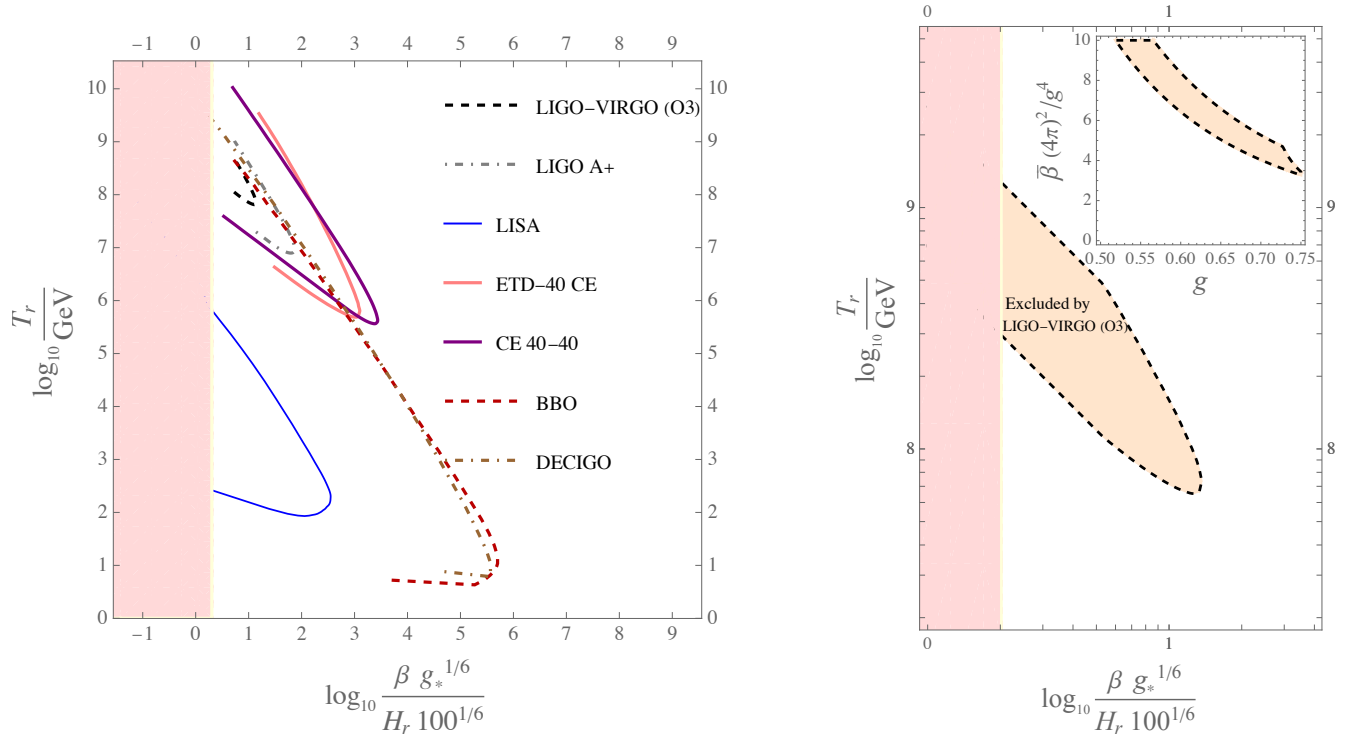


Figure 2: Regions where $\Omega_{\text{GW}}(f_{\text{peak}})$ is above the sensitivities of several current and proposed GW detectors. The shaded pink region to the left of the vertical straight line is the one forbidden by the BBN bound in (4.9). **Left plot:** For each curve, the region is the one obtained drawing semi-straight lines with derivative equal to -1 starting from all points of the curve and going to the left. **Right plot:** a zoom of the region corresponding to the LIGO-VIRGO third observing run (O3), which has therefore been excluded; the inset in the right plot shows the corresponding excluded region in the $\{g, \bar{\beta}\}$ space in the case of fast reheating (fixing $g_*(T_r) = 110$ and $\chi_0 = 2 \times 10^9 \text{ GeV}$)

Fig. 2 shows the regions where $\Omega_{\text{GW}}(f_{\text{peak}})$ is above the sensitivities of several current and proposed GW detectors: Advanced LIGO's and Advanced Virgo's third observing (O3) run (for power law-spectra), a possible upgrade of the current Advanced LIGO facilities (LIGO A+) [71, 72], LISA (power law sensitivity) [73], an ET array combined with a CE in the US (ETD-40 CE) and two CE detectors in the US with arm lengths of 40 km [74], BBO and DECIGO (for power law spectra) [75, 76]. In Fig. 2 it is also shown the bound in (4.9).

The region corresponding to the LIGO-VIRGO O3 is ruled out (a zoom of this region, computed for power-law spectra [71], is given in the right plot of Fig. 2), while the other regions, which is most of the parameter space, are still allowed as the corresponding observations have not yet been performed. The inset of the right plot of Fig. 2 shows the region excluded by the LIGO-VIRGO O3 in the $\{g, \bar{\beta}\}$ space in the case of fast reheating and fixing $g_*(T_r)$ and χ_0 to some reference values. The latter parameter has been chosen around 10^9 GeV because the corresponding f_{peak} is then around the frequency range of LIGO-VIRGO O3 [71] (see Fig. 4). The dependence on $g_*(T_r)$, on the other hand, is very weak. A χ_0 around 10^9 GeV is relevant e.g. for axion models. We checked that for all values of g and $\bar{\beta}$ in the inset of Fig. 2 the parameter ϵ in (3.16) is below one.

In Fig. 4 it is also shown f_{peak} for other values of χ_0 ; also in that figure we considered only

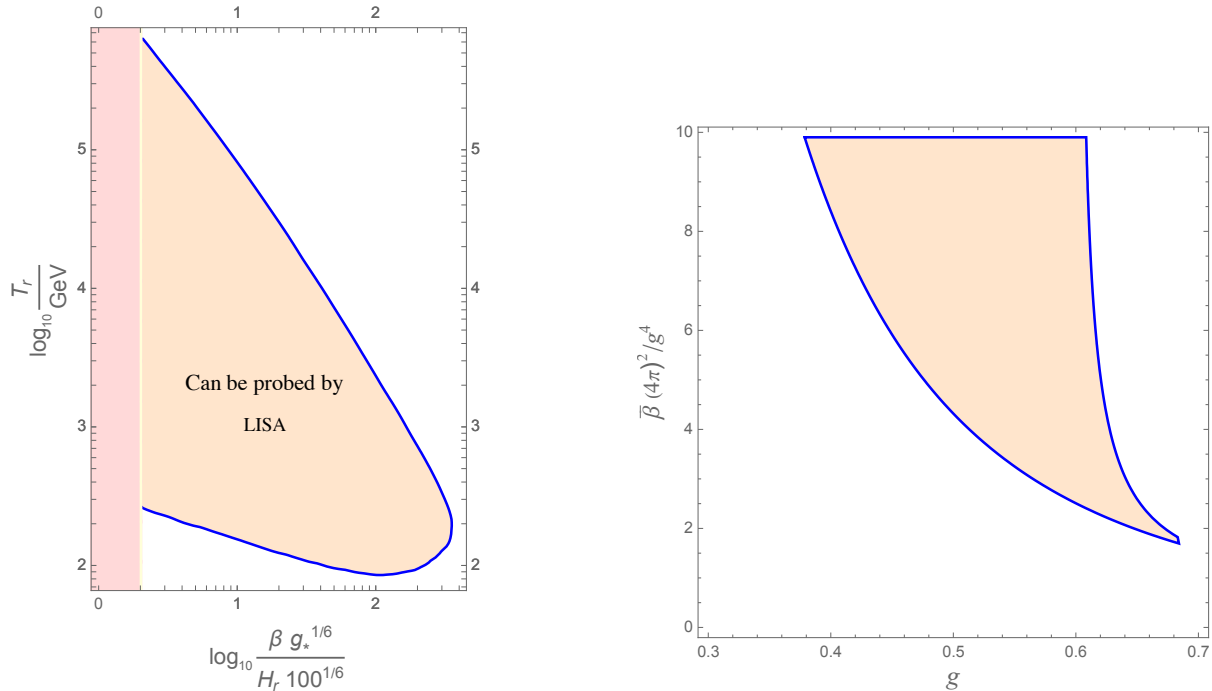


Figure 3: Like in the right plot of Fig. 2, but for LISA rather than LIGO-VIRGO O3 and fixing $g_*(T_r) = 110$ and $\chi_0 = 10^4$ GeV.

values of g and $\bar{\beta}$ such that ϵ is below one.

Using Fig. 4 one sees that when χ_0 is instead closer to the EW scale one will be able to probe this scenario through e.g. LISA, BBO and DECIGO (see Refs. [73, 75, 76]); higher values of χ_0 can instead be tested by ET and CE (see Ref. [74]). Given the phenomenological relevance of χ_0 close to the EW scale, in Fig. 3 it is shown the region of the parameter space that can be probed by LISA (with the same conventions as in the right plot of Fig. 2, but for LISA instead of LIGO-VIRGO O3 and also there we checked that for all values of g and $\bar{\beta}$ the quantity ϵ is below one). A χ_0 around 10 or 100 TeV is relevant for unified theories such as the Pati-Salam model [77] or Trinitification [78].

5 Improved approximations

The approximation performed in (3.17)-(3.18) generically corresponds to neglecting terms of order $\sqrt{\epsilon}$ (where ϵ is defined in (3.16)). Since we eventually need to set $T = T_n$, see Eq. (4.2), the approximation in (3.12) and dropping the $X \log X$ term in Eq. (3.25) for the nucleation temperature T_n , on the other hand, correspond to neglecting terms of relative order $(\log X)/X$, which are smaller than $\sqrt{\epsilon}$ because, since ϵ is small, $X \gtrsim g^4/(6\bar{\beta}) = \epsilon X$, which is large because $\bar{\beta}$ is loop suppressed⁶. What we are doing here is a small ϵ expansion (a “supercool expansion”) and

⁶The approximation in (3.12) consists in neglecting terms of relative order $1/X$ and $\log(\epsilon/g^2)/X$. The order of magnitude of the former is obviously not larger than $(\log X)/X$, but also that of the latter is so: apparently it might become larger than $(\log X)/X$ when $g \rightarrow 0$, but, as we have seen around (3.29), in this limit there is no solution for

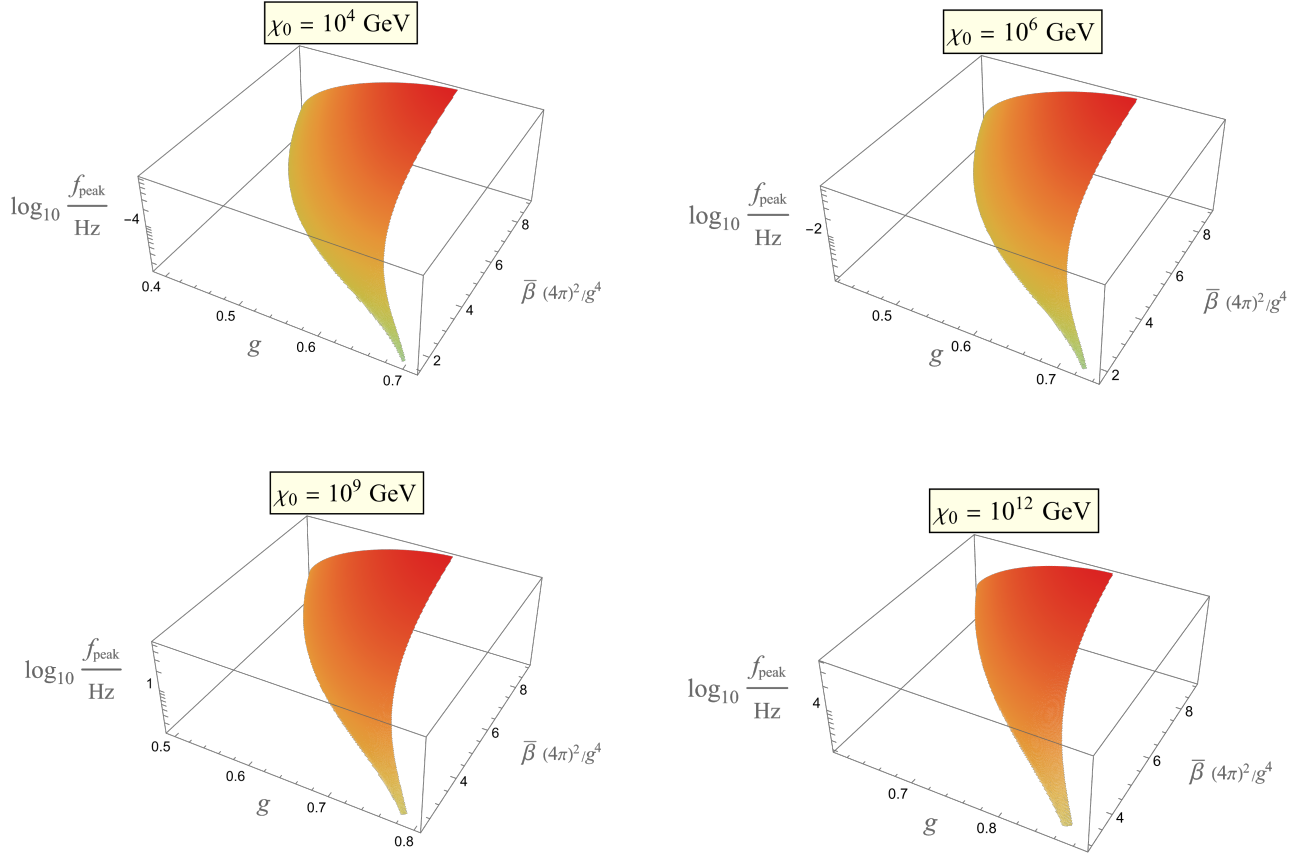


Figure 4: The peak frequency as a function of g and $\bar{\beta}$ in the case of fast reheating and fixing $g_*(T_r) = 110$.

what we have done so far is the analysis at leading order (LO), that is modulo terms of relative order $\sqrt{\epsilon}$. In this section we discuss how to improve the LO result by calculating higher-order corrections in the supercool expansion.

The first step is to calculate the corrections of relative order $\sqrt{\epsilon}$ with respect to the LO approximation, which corresponds to working at next-to-leading order in the supercool expansion (henceforth NLO). This can be done by improving the approximation in (3.17)-(3.18): including the term of order⁷ $x^{3/2}$ in the expansion of $J_B(x)$ in (2.24), one obtains

$$J_B(x) \approx J_B(0) + \frac{\pi^2}{12}x - \frac{\pi}{6}x^{3/2}, \quad (5.1)$$

$$J_F(x) \approx J_F(0) - \frac{\pi^2}{24}x. \quad (5.2)$$

Since for field values that are relevant for the bounce action x is at most of order ϵ (see Eqs. (3.15) and (2.23)), this corresponds to neglecting terms of order not larger than $\epsilon \log \epsilon$ relatively to the

⁷This term was overlooked in Ref. [45] (see Eq. (3) there).

LO. So the approximation in (3.12) and dropping terms of order $X \log X$ in the equation for the nucleation temperature are still valid even at NLO.

The effective potential at NLO, therefore, includes a term that is cubic in the field χ and reads

$$\bar{V}_{\text{eff}}(\chi, T) \approx \frac{m^2(T)}{2}\chi^2 - \frac{k(T)}{3}\chi^3 - \frac{\lambda(T)}{4}\chi^4 \quad (5.3)$$

where m^2 and λ are defined in (3.20),

$$k(T) \equiv \frac{\tilde{g}^3 T}{4\pi}, \quad (5.4)$$

and \tilde{g} is a non-negative real parameter defined by

$$\tilde{g}^3 \chi^3 \equiv \sum_b n_b m_b^3(\chi). \quad (5.5)$$

Here the m_b^3 are the cube of the background-dependent bosonic squared masses, which are all real, non-negative and proportional to χ . So \tilde{g}^3 is real, non-negative and independent of χ ; it is an extra parameter, which is needed to describe this scenario in a model-independent way at NLO. In general we have

$$\tilde{g} \leq g. \quad (5.6)$$

In order to understand why the term cubic in χ in (5.3) can be considered as a small correction in the supercool expansion, one can rescale $\chi \rightarrow \chi/\sqrt{\lambda}$ in the bounce action, Eq. (3.2), to obtain

$$S = \frac{4\pi}{\lambda} \int_0^{1/T} dt_E \left[\int_0^\infty dr r^2 \left(\frac{1}{2}\dot{\chi}^2 + \frac{1}{2}\chi'^2 + \frac{m^2}{2}\chi^2 - \frac{1}{4}\chi^4 \right) - \frac{k}{3\sqrt{\lambda}} \int_0^\infty dr r^2 \chi^3 \right]. \quad (5.7)$$

Since $\lambda = \bar{\beta} \log(\chi_0/T)$ and eventually we need to set $T = T_n$, we explicitly see that the term proportional to k has relative order at most $\sqrt{\epsilon}$ times a number smaller than one $\approx 1/(\sqrt{2}\pi)$ (where the LO result $S \approx 4\pi g T / (\sqrt{12}\lambda)$ and (5.6) have been used). This small number helps the convergence of the supercool expansion. Working at NLO, we can substitute χ with the solution of the unperturbed (that is LO) bounce problem both in the second integral in the square bracket (because suppressed by $\sqrt{\epsilon}$) and in the first one (because the first variation of the action around a solution of the field equations vanishes). So one obtains

$$S_3 = \frac{1}{\lambda} \left(c_3 m - \tilde{c}_3 \frac{k}{3\sqrt{\lambda}} \right), \quad (5.8)$$

where c_3 is given in Eq. (3.22),

$$\tilde{c}_3 \equiv 4\pi \int_0^\infty dr r^2 \chi_{\text{LO}}^3 \quad (5.9)$$

and χ_{LO} is the LO bounce configuration. A numerical calculation then gives $\tilde{c}_3 = 31.6915\dots$. Again, like in Eq. (3.22), we find a quite large value because of the geometrical factor of 4π overall.

Having obtained the NLO bounce action we can now improve the LO equation in (3.28) which gives T_n . Using (3.23), which holds at all orders in the supercool expansion, one obtains

$$\frac{3}{2}X \log X - \frac{3}{2}X \log \left(1 - \frac{\delta}{a\sqrt{X}} \right) \approx cX - 4X^2 - a + \frac{\delta}{\sqrt{X}}, \quad (5.10)$$

where a and c are defined in (3.27) and

$$\delta \equiv \frac{\tilde{c}_3 \tilde{g}^3}{12\pi \tilde{\beta}^{3/2}}. \quad (5.11)$$

Using (5.6), the quantity $\frac{\delta}{a\sqrt{X}}$ turns out to be at most of order $\sqrt{\epsilon}$. So, working at NLO, we can drop both terms on the left-hand side of (5.10), which are of relative order $(\log X)/X$ or smaller, and obtain

$$-\frac{\delta}{\sqrt{X}} \approx cX - 4X^2 - a. \quad (5.12)$$

Now, to find a solution one can again proceed perturbatively: calling X_{LO} the LO solution, namely

$$X_{\text{LO}} = \frac{c - \sqrt{c^2 - 16a}}{8}, \quad (5.13)$$

the NLO solution can be obtained by substituting X with X_{LO} only in the left-hand side of Eq. (5.12) and then solving with respect to X . This leads to the following NLO solution for T_n :

$$T_n \approx \chi_0 \exp\left(\frac{\sqrt{c^2 - 16(a - \delta/\sqrt{X_{\text{LO}}})} - c}{8}\right). \quad (5.14)$$

Let us now determine the NLO expression for β/H_n , Eq. (4.2). To this purpose it is useful to write

$$\frac{S_3}{T} = \frac{a}{\log \frac{\chi_0}{T}} \left(1 - \frac{\delta/a}{\sqrt{\log \frac{\chi_0}{T}}}\right). \quad (5.15)$$

Inserting now in (4.2) and dropping terms of relative order smaller than ϵ , which are negligible even at NLO,

$$\frac{\beta}{H_n} \approx \frac{a}{\log^2(\chi_0/T_n)} \left(1 - \frac{3\delta/a}{2\sqrt{\log(\chi_0/T_n)}}\right) - 4. \quad (5.16)$$

Note that, interestingly, the NLO correction reduces β and so renders Ω_{GW} larger, see Eq. (4.6).

In Fig. 5 we show the regions where $\Omega_{\text{GW}}(f_{\text{peak}})$ is above the sensitivities of LIGO-VIRGO O3 (left plot) and LISA (right plot) for two non-vanishing values of \tilde{g} . These plots should be compared respectively with the inset in Fig. 2 and with the right plot in 3 (which have instead $\tilde{g} \approx 0$). Note that a value of \tilde{g} much smaller than g is possible: it can happen in models where there are several particles with comparable values of their couplings to χ . In Fig. 5 we considered only values of g and $\tilde{\beta}$ such that ϵ (computed at LO) is below one.

One can then go ahead with this expansion. The next step, the next-to-next-to-leading order (NNLO), would consist in including terms of order $\epsilon \log \epsilon$ and ϵ . This would require including the $x^2 \log x$ and x^2 terms in the small- x expansion of $J_B(x)$ and $J_F(x)$, Eqs. (2.24)-(2.25), and considering the field-dependent logarithm in (3.11). Consequently also the $X \log X$ and X terms in the left-hand side of Eq. (5.10) for the nucleation temperature T_n (which needs to be corrected at NNLO) should be considered. In doing these improvements one would need to include extra parameters related to the fourth powers and the logarithms of the couplings of all fields to χ . Because of the small numbers in front of $x^2 \log x$ terms in Eqs. (2.24)-(2.25) and the fact that the terms $\log(\chi_b/T) - 1/4$ in (3.11) are at most of order $\log X/X < \epsilon \log \epsilon$ (relatively to the LO)

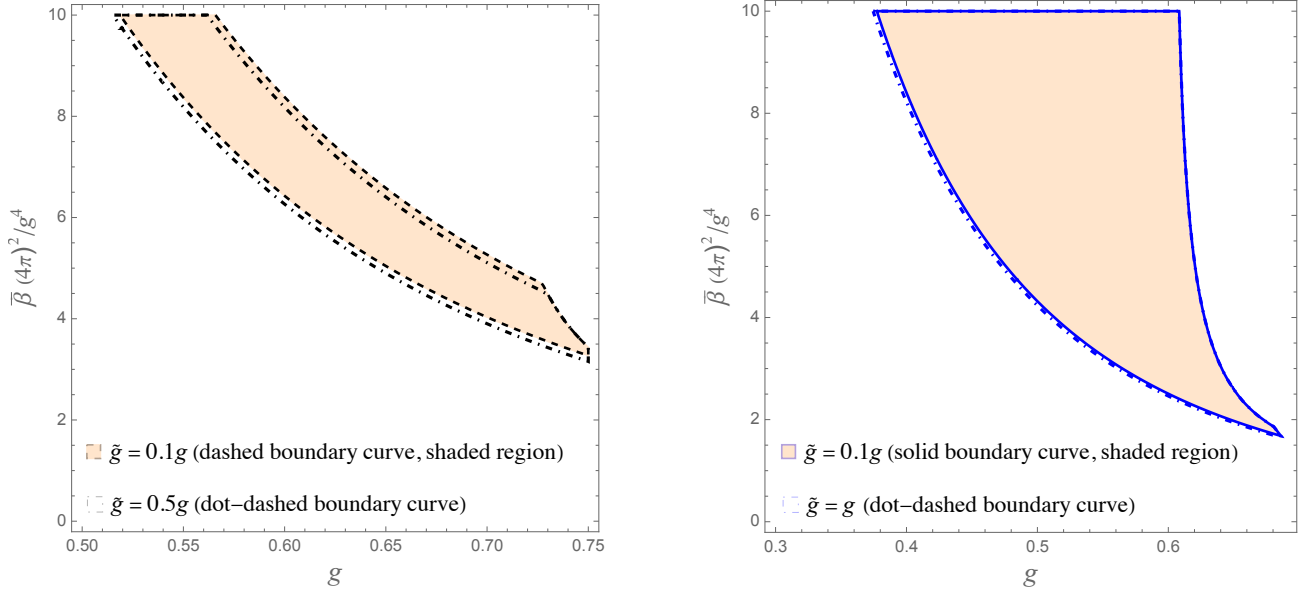


Figure 5: *Regions where $\Omega_{\text{GW}}(f_{\text{peak}})$ is above the sensitivities of LIGO-VIRGO O3 (left plot, where $\chi_0 = 2 \times 10^9 \text{ GeV}$) and LISA (right plot, where $\chi_0 = 10^4 \text{ GeV}$) computed at NLO in the supercool expansion. In both plots $g_*(T_r) = 110$ and fast reheating is assumed.*

one expects that their inclusion would generically lead to tiny corrections as long as ϵ is small. A complete analysis of the NNLO and higher orders goes beyond this work and is left for future activities.

6 Summary and conclusions

Let us start this final section with a summary of the main original results of this paper.

- To begin with, in Sec. 2 it has been shown that in an arbitrary RSB scenario (where symmetries are broken and masses are generated mostly by perturbative radiative effects) the one-loop effective potential, which has been computed explicitly and includes both quantum and thermal contributions, is always real as long as the classical potential is bounded from below. This an important starting point to establish the validity of the loop expansion.
- The PT of any RSB model is of first order when analyzed with perturbative methods as shown in Sec. 3.1. However, in Sec. 3.2 it has then been proved that, for our purposes, one can trade the hypothesis of perturbativity with that of supercooling (together with, of course, that of small-enough couplings) to obtain that the symmetric and asymmetric configurations, $\chi = 0$ and $\chi = \chi_0$, are always separated by a barrier for the relevant temperatures, $T \ll \chi_0$.
- Sec. 3.2 contains other very important results. There it has been shown that if supercooling is large enough, namely if ϵ defined in (3.16) is small, a model-independent description of the first-order phase transition is possible in terms of the following key parameters.

- χ_0 : the symmetry breaking scale
- $\bar{\beta}$: the beta function of the quartic coupling λ_χ of the flat-direction field χ , evaluated at the scale where $\lambda_\chi = 0$.
- g : a sort of collective coupling of χ to all fields of the theory, which is precisely defined in Eq. (3.9). It is basically the square root of the sum of the squares of the couplings of χ to all fields.

These parameters can be computed and the smallness of ϵ can be checked once the model is specified. As discussed in Sec. 3.2, when the theory is perturbative and, thus, approximately scale invariant, a large amount of cooling is always present [45], and consequently the PT is strongly of first order, but here it has been found that, for the model-independent approach to work, having a small ϵ is important⁸.

In the same section the validity of the one-loop approximation and the derivative expansion has been shown to follow from the hypothesis of supercooling, together with, of course, the requirement of small-enough couplings. This provides an extra motivation for considering the RSB scenario. In general, the gravitational contribution to the tunneling process turns out to be negligible for $\chi_0 \ll M_P$. Moreover, we have shown that the tunneling process is always dominated by the time-independent bounce as long as ϵ is small.

- The description of the PT in terms of only χ_0 , $\bar{\beta}$ and g is a leading order (LO) approximation in a small ϵ (supercool) expansion. The smaller ϵ the more accurate this approximation is; in general the errors associated with the LO approximation are of relative order not larger than $\sqrt{\epsilon}$ (see Sec. 5), but can even be smaller in specific setups. A next-to-leading (NLO) approximation can be obtained by including one more parameter, \tilde{g} , precisely defined in (5.5). This parameter is basically the cube root of the sum of the cubes of the couplings of χ to all bosonic fields, so $\tilde{g} \leq g$. Just like χ_0 , $\bar{\beta}$ and g , the extra parameter \tilde{g} can be computed once the model is specified. The NLO approximation should describe any RSB model modulo terms of relative order not larger than $\epsilon \log \epsilon$. One can improve even further the precision by going to the next-to-next-leading order (NNLO), by including additional parameters, as it is natural to expect. These results regarding the accuracy of the approximations and the supercool expansion are provided in Sec. 5. In that section we have also computed the bounce action, a key ingredient to study the PT, as well as the nucleation temperature T_n and the inverse duration of the PT, β , at NLO.
- In Secs. 4 and 5 the corresponding GW spectrum is studied and compared with the experimental results and the expected sensitivities of current and future GW detectors, to find regions of the parameter space that are either already ruled out or can lead to a future detection. If reheating is fast, the spectrum can be described at LO by χ_0 , $\bar{\beta}$ and g only (with a weak dependence on the effective number of relativistic species g_*); in going to NLO one adds the extra parameter \tilde{g} . If reheating is not fast one should also include the reheating temperature and the corresponding Hubble rate among the independent parameters, but for

⁸A non-perturbative way to realize a quasi-scale invariant scenario for PTs, on the other hand, is to use the AdS/CFT correspondence (see e.g. [80–83]). Also in these models supercooling occurs and the phase transition lasts a long time. The advantage of the perturbative scenario discussed here is the possibility of a model-independent description (at least for a large-enough supercooling), which has not (yet) been established at the non-perturbative level.

a fast reheating these are dependent on the previously-mentioned parameters. Interestingly, a large supercooling (ϵ small), which allows us to obtain a model-independent description, also generically increases the duration of the PT and makes it more likely for these GW signals to be observed in the future.

- It is also important to mention that the LO and NLO approximations have been carried out analytically in terms of the key parameters, χ_0 , $\bar{\beta}$ and g , as well as \tilde{g} for the NLO approximation. This allows to easily compute the key quantities of PTs and GW spectra in a supercool expansion once the model is specified.

To conclude, in this work we constructed a model-independent approach to RSB and the consequent PTs and GW spectra when enough supercooling occurs and we established the accuracy of such approach working at LO and NLO in the supercool expansion. The analytical formulæ produced in the paper are ready to be used in specific models and setups to avoid repeating the study of the PTs and GW spectra. The detailed analysis at higher orders, starting from the NNLO, is another possible outlook for future work.

Acknowledgments

I thank Giuliano Panico and Michele Redi for useful correspondence. This work has been partially supported by the grant DyConn from the University of Rome Tor Vergata.

References

- [1] B. P. Abbott *et al.* [LIGO Scientific and Virgo Collaborations], “Observation of Gravitational Waves from a Binary Black Hole Merger,” *Phys. Rev. Lett.* **116**, 061102 (2016) doi:10.1103/PhysRevLett.116.061102 [arXiv:1602.03837].
- [2] B. Abbott *et al.* [LIGO Scientific and Virgo], “GW150914: Implications for the stochastic gravitational wave background from binary black holes,” *Phys. Rev. Lett.* **116**, no.13, 131102 (2016) doi:10.1103/PhysRevLett.116.131102 [arXiv:1602.03847].
- [3] B. P. Abbott *et al.* “Multi-messenger Observations of a Binary Neutron Star Merger,” *Astrophys. J. Lett.* **848** (2017) no.2, L12 doi:10.3847/2041-8213/aa91c9 [arXiv:1710.05833].
- [4] M. Maggiore, “Gravitational Waves. Vol. 2: Astrophysics and Cosmology,” Oxford University Press, 3, 2018.
- [5] S. Weinberg, “Gauge and Global Symmetries at High Temperature,” *Phys. Rev. D* **9** (1974), 3357-3378 doi:10.1103/PhysRevD.9.3357
- [6] S. R. Coleman and E. J. Weinberg, “Radiative Corrections as the Origin of Spontaneous Symmetry Breaking,” *Phys. Rev. D* **7** (1973), 1888-1910 doi:10.1103/PhysRevD.7.1888
- [7] N. Levi, T. Opferkuch and D. Redigolo, “The Supercooling Window at Weak and Strong Coupling,” [arXiv:2212.08085].
- [8] E. Gildener and S. Weinberg, “Symmetry Breaking and Scalar Bosons,” *Phys. Rev. D* **13** (1976), 3333 doi:10.1103/PhysRevD.13.3333
- [9] J. R. Espinosa, T. Konstandin, J. M. No and M. Quiros, “Some Cosmological Implications of Hidden Sectors,” *Phys. Rev. D* **78** (2008), 123528 doi:10.1103/PhysRevD.78.123528 [arXiv:0809.3215].
- [10] A. Farzinnia and J. Ren, “Strongly First-Order Electroweak Phase Transition and Classical Scale Invariance,” *Phys. Rev. D* **90** (2014)

- no.7, 075012 doi:10.1103/PhysRevD.90.075012 [arXiv:1408.3533].
- [11] F. Sannino and J. Virkajärvi, “First Order Electroweak Phase Transition from (Non)Conformal Extensions of the Standard Model,” *Phys. Rev. D* **92** (2015) no.4, 045015 doi:10.1103/PhysRevD.92.045015 [arXiv:1505.05872].
- [12] L. Marzola, A. Racioppi and V. Vaskonen, “Phase transition and gravitational wave phenomenology of scalar conformal extensions of the Standard Model,” *Eur. Phys. J. C* **77** (2017) no.7, 484 doi:10.1140/epjc/s10052-017-4996-1 [arXiv:1704.01034].
- [13] V. Brdar, A. J. Helmboldt and M. Lindner, “Strong Supercooling as a Consequence of Renormalization Group Consistency,” *JHEP* **12** (2019), 158 doi:10.1007/JHEP12(2019)158 [arXiv:1910.13460].
- [14] M. Kierkla, A. Karam and B. Swiezevska, “Conformal model for gravitational waves and dark matter: A status update,” [arXiv:2210.07075].
- [15] W. C. Huang, F. Sannino and Z. W. Wang, “Gravitational Waves from Pati-Salam Dynamics,” *Phys. Rev. D* **102**, no.9, 095025 (2020) doi:10.1103/PhysRevD.102.095025 [arXiv:2004.02332].
- [16] R. D. Peccei and H. R. Quinn, “CP Conservation in the Presence of Instantons,” *Phys. Rev. Lett.* **38** (1977), 1440-1443 doi:10.1103/PhysRevLett.38.1440. R. D. Peccei and H. R. Quinn, “Constraints Imposed by CP Conservation in the Presence of Instantons,” *Phys. Rev. D* **16** (1977) 1791 doi:10.1103/PhysRevD.16.1791
- [17] L. Delle Rose, G. Panico, M. Redi and A. Tesi, “Gravitational Waves from Supercool Axions,” *JHEP* **04** (2020), 025 doi:10.1007/JHEP04(2020)025 [arXiv:1912.06139].
- [18] B. Von Harling, A. Pomarol, O. Pujolàs and F. Rompineve, “Peccei-Quinn Phase Transition at LIGO,” *JHEP* **04** (2020), 195 doi:10.1007/JHEP04(2020)195 [arXiv:1912.07587].
- [19] A. Salvio, “A fundamental QCD axion model,” *Phys. Lett. B* **808** (2020), 135686 doi:10.1016/j.physletb.2020.135686 [arXiv:2003.10446].
- [20] A. Ghoshal and A. Salvio, “Gravitational waves from fundamental axion dynamics,” *JHEP* **12** (2020), 049 doi:10.1007/JHEP12(2020)049 [arXiv:2007.00005].
- [21] V. Brdar, A. J. Helmboldt and J. Kubo, “Gravitational Waves from First-Order Phase Transitions: LIGO as a Window to Unexplored Seesaw Scales,” *JCAP* **02** (2019), 021 doi:10.1088/1475-7516/2019/02/021 [arXiv:1810.12306].
- [22] J. Kubo, J. Kuntz, M. Lindner, J. Rezaeck, P. Saake and A. Trautner, “Unified emergence of energy scales and cosmic inflation,” *JHEP* **08** (2021), 016 doi:10.1007/JHEP08(2021)016 [arXiv:2012.09706].
- [23] A. Salvio, “Dimensional Transmutation in Gravity and Cosmology,” *Int. J. Mod. Phys. A* **36** (2021) no.08n09, 2130006 doi:10.1142/S0217751X21300064 [arXiv:2012.11608].
- [24] G. M. Harry [LIGO Scientific], “Advanced LIGO: The next generation of GW detectors,” *Class. Quant. Grav.* **27**, 084006 (2010) doi:10.1088/0264-9381/27/8/084006
- [25] J. Aasi *et al.* [LIGO Scientific], “Advanced LIGO,” *Class. Quant. Grav.* **32**, 074001 (2015) doi:10.1088/0264-9381/32/7/074001 [arXiv:1411.4547].
- [26] F. Acernese *et al.* [VIRGO], “Advanced Virgo: a second-generation interferometric gravitational wave detector,” *Class. Quant. Grav.* **32** (2015) no.2, 024001 doi:10.1088/0264-9381/32/2/024001 [arXiv:1408.3978].
- [27] B. P. Abbott *et al.* [LIGO Scientific], “Exploring the Sensitivity of Next Generation Gravitational Wave Detectors,” *Class. Quant. Grav.* **34**, no.4, 044001 (2017) doi:10.1088/1361-6382/aa51f4 [arXiv:1607.08697].

- [28] D. Reitze *et al.*, “Cosmic Explorer: The U.S. Contribution to Gravitational-Wave Astronomy beyond LIGO,” *Bull. Am. Astron. Soc.* **51**, 035 [[arXiv:1907.04833](#)].
- [29] M. Punturo *et al.*, “The Einstein Telescope: A third-generation GW observatory,” *Class. Quant. Grav.* **27**, 194002 (2010) doi:10.1088/0264-9381/27/19/194002
- [30] S. Hild *et al.*, “Sensitivity Studies for Third-Generation Gravitational Wave Observatories,” *Class. Quant. Grav.* **28**, 094013 (2011) doi:10.1088/0264-9381/28/9/094013 [[arXiv:1012.0908](#)].
- [31] B. Sathyaprakash *et al.*, “Scientific Objectives of Einstein Telescope,” *Class. Quant. Grav.* **29**, 124013 (2012) doi:10.1088/0264-9381/29/12/124013 [[arXiv:1206.0331](#)].
- [32] J. Crowder and N. J. Cornish, “Beyond LISA: Exploring future GW missions,” *Phys. Rev. D* **72**, 083005 (2005) doi:10.1103/PhysRevD.72.083005 [[arXiv:gr-qc/0506015](#)].
- [33] V. Corbin and N. J. Cornish, “Detecting the cosmic GW background with the big bang observer,” *Class. Quant. Grav.* **23**, 2435-2446 (2006) doi:10.1088/0264-9381/23/7/014 [[arXiv:gr-qc/0512039](#)].
- [34] G. Harry, P. Fritschel, D. Shaddock, W. Folkner and E. Phinney, “Laser interferometry for the big bang observer,” *Class. Quant. Grav.* **23**, 4887-4894 (2006) doi:10.1088/0264-9381/23/15/008 [[arXiv:gr-qc/0506015](#)]
- [35] N. Seto, S. Kawamura and T. Nakamura, “Possibility of direct measurement of the acceleration of the universe using 0.1-Hz band laser interferometer GW antenna in space,” *Phys. Rev. Lett.* **87**, 221103 (2001) doi:10.1103/PhysRevLett.87.221103 [[arXiv:astro-ph/0108011](#)].
- [36] S. Kawamura *et al.*, “The Japanese space gravitational wave antenna - DECIGO,” *Class. Quant. Grav.* **23** (2006), S125-S132. doi:10.1088/0264-9381/23/8/S17
- [37] P. Amaro-Seoane *et al.* [LISA], “Laser Interferometer Space Antenna,” [[arXiv:1702.00786](#)].
- [38] Youla, D. C. (1961), “A normal Form for a Matrix under the Unitary Congruence Group”. *Can. J. Math.* **13**: 694-704. doi:10.4153/CJM-1961-059-8
- [39] L. Dolan and R. Jackiw, “Symmetry Behavior at Finite Temperature,” *Phys. Rev. D* **9** (1974), 3320-3341 doi:10.1103/PhysRevD.9.3320
- [40] S. R. Coleman, “The Fate of the False Vacuum. 1. Semiclassical Theory,” *Phys. Rev. D* **15** (1977), 2929-2936 [erratum: *Phys. Rev. D* **16** (1977), 1248] doi:10.1103/PhysRevD.16.1248
- [41] C. G. Callan, Jr. and S. R. Coleman, “The Fate of the False Vacuum. 2. First Quantum Corrections,” *Phys. Rev. D* **16** (1977), 1762-1768 doi:10.1103/PhysRevD.16.1762
- [42] A. D. Linde, “Fate of the False Vacuum at Finite Temperature: Theory and Applications,” *Phys. Lett. B* **100** (1981), 37-40 doi:10.1016/0370-2693(81)90281-1
- [43] A. D. Linde, “Decay of the False Vacuum at Finite Temperature,” *Nucl. Phys. B* **216** (1983), 421. Erratum: [*Nucl. Phys. B* **223**, 544 (1983)] doi:10.1016/0550-3213(83)90072-X
- [44] S. R. Coleman, V. Glaser and A. Martin, “Action Minima Among Solutions to a Class of Euclidean Scalar Field Equations,” *Commun. Math. Phys.* **58** (1978), 211-221 doi:10.1007/BF01609421
- [45] E. Witten, “Cosmological Consequences of a Light Higgs Boson,” *Nucl. Phys. B* **177** (1981), 477-488 doi:10.1016/0550-3213(81)90182-6
- [46] A. D. Linde, “Phase Transitions in Gauge Theories and Cosmology,” *Rept. Prog. Phys.* **42**, 389 (1979) doi:10.1088/0034-4885/42/3/001
- [47] A. D. Linde, “Infrared Problem in Thermodynamics of the Yang-Mills Gas,” *Phys. Lett. B* **96**, 289-292 (1980) doi:10.1016/0370-2693(80)90769-8
- [48] A. Salvio, A. Strumia, N. Tetradis and A. Urbano, “On gravitational and thermal corrections to vacuum decay,” *JHEP* **09** (2016), 054 doi:10.1007/JHEP09(2016)054 [[arXiv:1608.02555](#)].
- [49] E. Brezin and G. Parisi, *J. Stat. Phys.* **19** (1978) 269 doi:10.1007/BF01011726

- [50] P. B. Arnold and S. Vokos, “Instability of hot electroweak theory: bounds on $m(H)$ and $M(t)$,” *Phys. Rev. D* **44** (1991), 3620-3627 doi:10.1103/PhysRevD.44.3620
- [51] J. Kearney, H. Yoo and K. M. Zurek, “Is a Higgs Vacuum Instability Fatal for High-Scale Inflation?,” *Phys. Rev. D* **91** (2015) no.12, 123537 doi:10.1103/PhysRevD.91.123537 [arXiv:1503.05193].
- [52] A. Joti, A. Katsis, D. Loupas, A. Salvio, A. Strumia, N. Tetradis and A. Urbano, “(Higgs) vacuum decay during inflation,” *JHEP* **07** (2017), 058 doi:10.1007/JHEP07(2017)058 [arXiv:1706.00792].
- [53] T. Markkanen, A. Rajantie and S. Stopyra, “Cosmological Aspects of Higgs Vacuum Metastability,” *Front. Astron. Space Sci.* **5** (2018), 40 doi:10.3389/fspas.2018.00040 [arXiv:1809.06923].
- [54] C. Caprini, M. Chala, G. C. Dorsch, M. Hindmarsh, S. J. Huber, T. Konstandin, J. Kozaczuk, G. Nardini, J. M. No and K. Rummukainen, *et al.* “Detecting gravitational waves from cosmological phase transitions with LISA: an update,” *JCAP* **03** (2020), 024 doi:10.1088/1475-7516/2020/03/024 [arXiv:1910.13125].
- [55] J. Ellis, M. Lewicki, J. M. No and V. Vaskonen, “Gravitational wave energy budget in strongly supercooled phase transitions,” *JCAP* **06** (2019), 024 doi:10.1088/1475-7516/2019/06/024 [arXiv:1903.09642].
- [56] C. Caprini, M. Hindmarsh, S. Huber, T. Konstandin, J. Kozaczuk, G. Nardini, J. M. No, A. Petiteau, P. Schwaller, G. Servant and D. J. Weir, “Science with the space-based interferometer eLISA. II: GWs from cosmological phase transitions,” *JCAP* **04** (2016), 001 doi:10.1088/1475-7516/2016/04/001 [arXiv:1512.06239].
- [57] M. Lewicki and V. Vaskonen, “Gravitational waves from bubble collisions and fluid motion in strongly supercooled phase transitions,” *Eur. Phys. J. C* **83** (2023) no.2, 109 doi:10.1140/epjc/s10052-023-11241-3 [arXiv:2208.11697].
- [58] C. Caprini and D. G. Figueroa, “Cosmological Backgrounds of Gravitational Waves,” *Class. Quant. Grav.* **35** (2018) no.16, 163001 doi:10.1088/1361-6382/aac608 [arXiv:1801.04268].
- [59] B. Von Harling, A. Pomarol, O. Pujolàs and F. Rompineve, “Peccei-Quinn Phase Transition at LIGO,” *JHEP* **04** (2020), 195 doi:10.1007/JHEP04(2020)195 [arXiv:1912.07587].
- [60] S. J. Huber and T. Konstandin, “Gravitational Wave Production by Collisions: More Bubbles,” *JCAP* **09** (2008), 022 doi:10.1088/1475-7516/2008/09/022 [arXiv:0806.1828].
- [61] K. Freese and M. W. Winkler, “Have pulsar timing arrays detected the hot big bang: Gravitational waves from strong first order phase transitions in the early Universe,” *Phys. Rev. D* **106** (2022) no.10, 103523 doi:10.1103/PhysRevD.106.103523 [arXiv:2208.03330].
- [62] R. Jinno and M. Takimoto, “Gravitational waves from bubble dynamics: Beyond the Envelope,” *JCAP* **01** (2019), 060 doi:10.1088/1475-7516/2019/01/060 [arXiv:1707.03111].
- [63] T. Konstandin, “Gravitational radiation from a bulk flow model,” *JCAP* **03** (2018), 047 doi:10.1088/1475-7516/2018/03/047 [arXiv:1712.06869].
- [64] M. Lewicki and V. Vaskonen, “On bubble collisions in strongly supercooled phase transitions,” *Phys. Dark Univ.* **30** (2020), 100672 doi:10.1016/j.dark.2020.100672 [arXiv:1912.00997].
- [65] M. Lewicki and V. Vaskonen, “Gravitational wave spectra from strongly supercooled phase transitions,” *Eur. Phys. J. C* **80** (2020) no.11, 1003 doi:10.1140/epjc/s10052-020-08589-1 [arXiv:2007.04967].
- [66] M. Lewicki and V. Vaskonen, “Gravitational waves from colliding vacuum bubbles in gauge theories,” *Eur. Phys. J. C* **81** (2021) no.5, 437 [erratum: *Eur. Phys. J. C* **81** (2021) no.12, 1077] doi:10.1140/epjc/s10052-021-09232-3 [arXiv:2012.07826].

- [67] L. A. Boyle and A. Buonanno, “Relating gravitational wave constraints from primordial nucleosynthesis, pulsar timing, laser interferometers, and the CMB: Implications for the early Universe,” *Phys. Rev. D* **78** (2008), 043531 doi:10.1103/PhysRevD.78.043531 [arXiv:0708.2279].
- [68] A. Stewart and R. Brandenberger, “Observational Constraints on Theories with a Blue Spectrum of Tensor Modes,” *JCAP* **08** (2008), 012 doi:10.1088/1475-7516/2008/08/012 [arXiv:0711.4602].
- [69] K. Kohri and T. Terada, “Semianalytic calculation of gravitational wave spectrum nonlinearly induced from primordial curvature perturbations,” *Phys. Rev. D* **97** (2018) no.12, 123532 doi:10.1103/PhysRevD.97.123532 [arXiv:1804.08577].
- [70] N. Aghanim *et al.* [Planck], “Planck 2018 results. VI. Cosmological parameters,” *Astron. Astrophys.* **641** (2020), A6 [erratum: *Astron. Astrophys.* **652** (2021), C4] doi:10.1051/0004-6361/201833910 [arXiv:1807.06209].
- [71] R. Abbott *et al.* [KAGRA, Virgo and LIGO Scientific], “Upper limits on the isotropic gravitational-wave background from Advanced LIGO and Advanced Virgo’s third observing run,” *Phys. Rev. D* **104** (2021) no.2, 022004 doi:10.1103/PhysRevD.104.022004 [arXiv:2101.12130].
- [72] R. Abbott *et al.* [LIGO Scientific, VIRGO and KAGRA], “Open data from the third observing run of LIGO, Virgo, KAGRA and GEO,” [arXiv:2302.03676].
- [73] S. Babak, A. Petiteau and M. Hewitson, “LISA Sensitivity and SNR Calculations,” [arXiv:2108.01167].
- [74] M. Evans, R. X. Adhikari, C. Afle, S. W. Ballmer, S. Biscoveanu, S. Borhanian, D. A. Brown, Y. Chen, R. Eisenstein and A. Gruson, *et al.* “A Horizon Study for Cosmic Explorer: Science, Observatories, and Community,” [arXiv:2109.09882].
- [75] E. Thrane and J. D. Romano, “Sensitivity curves for searches for gravitational-wave backgrounds,” *Phys. Rev. D* **88** (2013) no.12, 124032 [arXiv:1310.5300].
- [76] P. S. B. Dev, F. Ferrer, Y. Zhang and Y. Zhang, “Gravitational Waves from First-Order Phase Transition in a Simple Axion-Like Particle Model,” *JCAP* **11** (2019), 006 [arXiv:1905.00891].
- [77] J. C. Pati and A. Salam, “Lepton Number as the Fourth Color,” *Phys. Rev. D* **10** (1974), 275-289 [erratum: *Phys. Rev. D* **11** (1975), 703-703] doi:10.1103/PhysRevD.10.275
- [78] K. S. Babu, X. G. He and S. Pakvasa, “Neutrino Masses and Proton Decay Modes in SU(3) X SU(3) X SU(3) Trinification,” *Phys. Rev. D* **33** (1986), 763 doi:10.1103/PhysRevD.33.763
- [79] M. Quiros, “Field theory at finite temperature and phase transitions,” *Helv. Phys. Acta* **67** (1994) 451 doi:10.5169/seals-116659.
- [80] P. Creminelli, A. Nicolis and R. Rattazzi, “Holography and the electroweak phase transition,” *JHEP* **03**, 051 (2002) doi:10.1088/1126-6708/2002/03/051 [arXiv:hep-th/0107141].
- [81] L. Randall and G. Servant, “Gravitational waves from warped spacetime,” *JHEP* **05**, 054 (2007) doi:10.1088/1126-6708/2007/05/054 [arXiv:hep-ph/0607158].
- [82] G. Nardini, M. Quiros and A. Wulzer, “A Confining Strong First-Order Electroweak Phase Transition,” *JHEP* **09**, 077 (2007) doi:10.1088/1126-6708/2007/09/077 [arXiv:0706.3388].
- [83] T. Konstandin and G. Servant, “Cosmological Consequences of Nearly Conformal Dynamics at the TeV scale,” *JCAP* **12**, 009 (2011) doi:10.1088/1475-7516/2011/12/009 [arXiv:1104.4791].